

Maximizing Pencil-Beam Pattern Performance in Metasurface Antennas Through Full-Wave Optimization

Original

Maximizing Pencil-Beam Pattern Performance in Metasurface Antennas Through Full-Wave Optimization / Zucchi, M.; Scarabosio, A.; Righero, M.; Giordanengo, G.; Verni, F.; Massagrande, C.; Vecchi, G.. - ELETTRONICO. - (2023), pp. 1605-1606. (Intervento presentato al convegno 2023 IEEE International Symposium on Antennas and Propagation and USNC-URSI Radio Science Meeting (USNC-URSI) tenutosi a Portland, OR, USA nel 23-28 July 2023) [10.1109/USNC-URSI52151.2023.10237613].

Availability:

This version is available at: 11583/2982051 since: 2023-10-04T11:18:03Z

Publisher:

IEEE

Published

DOI:10.1109/USNC-URSI52151.2023.10237613

Terms of use:

This article is made available under terms and conditions as specified in the corresponding bibliographic description in the repository

Publisher copyright

IEEE postprint/Author's Accepted Manuscript

©2023 IEEE. Personal use of this material is permitted. Permission from IEEE must be obtained for all other uses, in any current or future media, including reprinting/republishing this material for advertising or promotional purposes, creating new collecting works, for resale or lists, or reuse of any copyrighted component of this work in other works.

(Article begins on next page)

Maximizing Pencil-Beam Pattern Performance in Metasurface Antennas Through Full-Wave Optimization

M. Zucchi*, A. Scarabosio[†], M. Righero[†], G. Giordanengo[†], F. Verni[‡], C. Massagrande[‡], G. Vecchi*

*Department of Electronics and Telecommunications, Politecnico di Torino, Torino, Italy;
giuseppe.vecchi@polito.it

[†]Advanced Computing, Photonics & Electromagnetics (CPE), Fondazione LINKS, Torino, Italy;
andrea.scarabosio@linksfoundation.com

[‡]Huawei, Milan Research Center, Segrate (MI), Italy;
francesco.verni@huawei.com

Abstract—We propose a design and optimization scheme for metasurface antennas that decouples the antenna and the feeding structure to maximize the antenna performance. This approach uses 2.5D fast algorithms to simulate the large antenna, significantly decreasing the amount of time and complexity required compared to 3D full-wave simulations. The optimization process is designed to maximize the antenna efficiency within a pencil beam pattern mask with a predefined database of unit cells. We present numerical results of the 3D metasurface antenna model comparing our code with a commercial solver to demonstrate the effectiveness of our approach.

Index Terms—computational electromagnetics, layered media, fast methods, antenna optimization, metasurfaces.

I. INTRODUCTION

Metamaterials and metasurfaces have enabled the design of complex electromagnetic devices, such as antennas, with standard materials and fabrication technologies. These antennas possess unique properties like low-loss, high-gain broadside radiating capabilities which were not possible before [1]. Despite the challenge of full-wave analysis with commercial solvers, this is still possible when the effective area of the metasurface antenna is limited to a few wavelengths. However, when the antenna becomes larger, full-wave analysis becomes unfeasible.

Metasurface antennas have been revolutionized by advances in numerical methods, allowing for greater flexibility in terms of

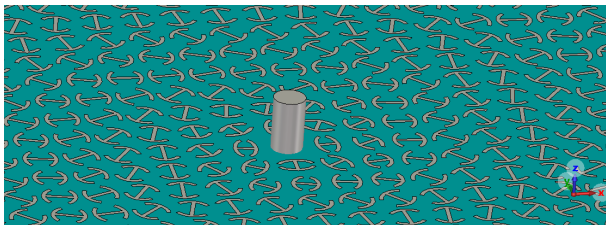


Fig. 1. A three dimensional view of the metasurface antenna around the coaxial feed.

radiation patterns and field requirements. These methods rely on integral equation formulations, discretized with well-known scattering problem techniques, such as equivalent electric currents expanded in terms of entire-domain basis functions [2]. In [3] the authors find the equivalent currents from radiated field mask-type requirements and obtains a 3D realizable metasurface via optimization. Global optimization techniques are used in [4], with the cost of the forward linear problem reduced by specialized entire-domain basis functions written as aggregation of local conventional Rao-Wilton-Glisson (RWG) basis functions. The accelerated algorithm design process used in this article is depicted in the chart in Fig. 2. The main feature is the separation of the 2D, but large, metasurface antenna and the 3D, but small in size, feeding system. These two parts are at first optimized separately, while the design is verified at the end with a fullwave simulation of the entire 3D antenna system. In Sec. II we briefly describe the different stages of the design and optimization process. In Sec. III we present numerical results of the 3D metasurface antenna model comparing our code with a commercial solver to demonstrate the effectiveness of our approach.

II. FAST FULL-WAVE DESIGN SCHEME

Creating a metasurface antenna from the optimal impedance profile requires a database of unit cell geometries that can generate the required impedance values. The parameters defining each unit-cell shape are varied within feasible ranges to create a database of impedance values. The synthesizable impedance values vary depending on the shape of the cell, with scalar values (e.g. circular patches) or tensorial values (e.g. double anchor, coffee bean, etc.). The impedance extraction method is taken from [5] and is applied to each individual geometry that populates the database. The bigger the database, the larger the space of optimal solutions. Each component of the continuous IBC profile is parameterized with N_p parameters, in order to reduce the effective number of degrees of freedom. The parametrization is dependent on the desired radiation pattern and can be chosen based on analytical consideration. For each

choice of the parameters, and therefore of the corresponding IBC profile, an objective value $f(\alpha_1, \alpha_2, \dots, \alpha_{N_p})$ is assigned to it by carrying out the following steps. First, the trial impedance profile is sampled on a regular grid of points corresponding to the unit cell locations. The impedance value is then projected onto the set of feasible values in the pre-computed database, using a fast nearest-neighbour search. With this realizable impedance profile, a new solution of the EFIE-IBC is obtained with the Method of Moments, employing acceleration methods (e.g., GIFFT). Then, the radiation is computed with fast methods and the error with respect to the prescribed FF masks gives the objective function value. Eventually, starting from the optimized impedance profile, each individual unit cell is selected by picking the proper geometrical parameters from the database. The solution is obtained by solving an EFIE problem to validate the radiation and efficiency properties.

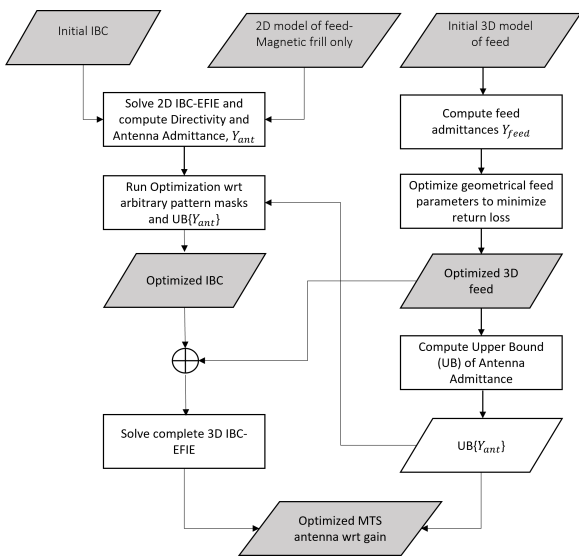


Fig. 2. Flow-chart of the accelerated design process.

III. THREE-DIMENSIONAL FULL-WAVE RESULTS

The considered geometry is a planar circular antenna of diameter $12\lambda = 16$ [cm], working at a frequency of 22.5 GHz. The dielectric substrate is the Panasonic Megtron-7 R-5785(N), it has a thickness of 0.508 [mm] and is placed over a ground plane. The database is populated of unit cell with a shape of a "double-anchor" as in Fig. 1, the distance between the centres of the unit cells is 2.2 [mm] $\approx \lambda/6$ in a cartesian lattice. The antenna is fed from the center by a vertical pin, as shown in Fig. 1. The radiation requirements are for a circularly polarized broadside beam, with cross-pol level at -25 dB. Side-lobe levels are set at -25 dB. The full structure of Fig. 1 has been analyzed together with the realistic feed structure in both CST microwave Studio 2023 and our code. In this way, the effect of the exciting structure is accurately modelled to get the realized gain of Fig. 3. To the best of our knowledge, the only solver that seems to provide stable solutions with this

kind of structure is the Time Domain Solver, which in our case results in about 268 million of hexahedral mesh cells. The resulting pattern are in agreement around the main lobe

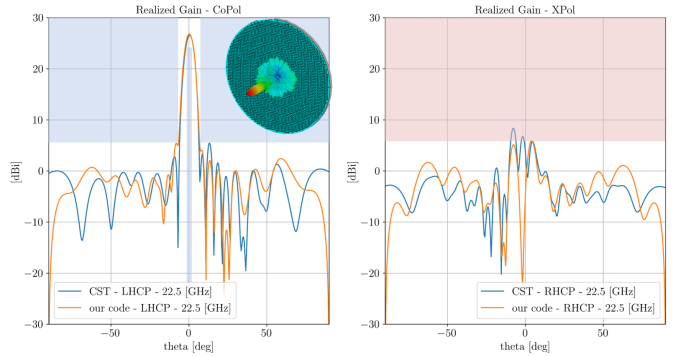


Fig. 3. Realized Gain of the metasurface antenna: co-pol (left) and x-pol (right) radiated by the antenna for $\theta \in [-90, 90]$ and $\phi = 0$. Blue solid lines refer to CST simulation, orange solid lines to our code. Blue and red shaded area represent the co-polar and cross-polar pattern mask used in the optimization process, respectively.

region for both the co- and cross-polarization, and remain well within the mask levels almost everywhere. The obtained design shows a maximum directivity of 27 dB, an aperture efficiency $\epsilon_{ap} \approx 38\%$, and a corresponding value of the reflection coefficient $S_{11} = -15.2$ dB.

IV. CONCLUSIONS

This article has presented a design and optimization process for 3D metasurface antennas. This process involves the separation of the 2D, but large, metasurface antenna and the 3D, but small in size, feeding system, which are optimized separately before being verified with a full-wave simulation of the entire 3D antenna system. Numerical results of the 3D metasurface antenna model which radiates with enhanced efficiency within pencil-beam pattern masks are presented, demonstrating the effectiveness of our approach when compared to a commercial solver. Measurements of the presented design will be shown at the conference.

REFERENCES

- [1] M. Faenzi, G. Minatti, D. González-Ovejero et al., "Metasurface antennas: new models, applications and realizations", in *Scientific Reports*, (2019) 9:10178
- [2] D. González-Ovejero and S. Maci, "Gaussian ring basis functions for the analysis of modulated metasurface antennas" *IEEE Trans. Antennas Propag.*, vol. 63, no. 9, pp. 3982–3993, Sep. 2015
- [3] G. Oliveri, P. Rocca, M. Salucci, and A. Massa, "Holographic Smart EM Skins for Advanced Beam Power Shaping in Next Generation Wireless Environments," *IEEE J. Multiscale Multiphysics Comput. Tech.*, vol. 6, pp. 171–182, 2021.
- [4] F. Verni, "Advanced Computational Electromagnetics for Metasurfaces," *Ph.D. dissertation*, Politecnico di Torino, Aug. 2020. [Online]. Available: <https://iris.polito.it/handle/11583/2843986?mode=simple.13517>
- [5] A. M. Patel and A. Grbic, "Modeling and Analysis of Printed-Circuit Tensor Impedance Surfaces," *IEEE Trans. Antennas Propag.*, vol. 61, no. 1, pp. 211–220, Jan. 2013.